Journal Name

ARTICLE

Observation of visible light activated photocatalytic degradation of stearic acid on thin films of tantalum oxynitride synthesized by aerosol assisted chemical vapour deposition

Received 00th January 20xx,
Accepted 00th January 20xx

DOI: 10.1039/x0xx00000x

www.rsc.org/

Samuel D. Cosham,[a] Veronica Celorrio[b, c] Alexander N Kulak,[d] and Geoffrey Hyett [a†]

UV activated photocatalysts deposited using chemical vapour deposition have found commercial success as self-cleaning coatings. However, only limited work has been conducted on the use of the more recently discovered visible light activated photocatalysis for this application. Tantalum oxynitride is an established visible light photocatalyst, and in this paper we have investigated the ability of thin films of tantalum oxynitride to photocatalytically degrade a model organic pollutant, stearic acid, and therefore assess the coatings potential for self-cleaning applications. Thin films of tantalum oxide were formed using aerosol assisted chemical vapour deposition (AACVD) of tantalum ethoxide, and then converted into tantalum oxynitride through ammonolysis at temperatures between 550 °C and 750 °C. Investigation of the films using XRD, UV-vis spectroscopy and XAFS identify that amorphous tantalum oxynitride is formed during the ammonolysis, with complete conversion to TaON under conditions of 700 °C for 24 hours. The self-cleaning ability of this film was assessed using stearic acid as the model pollutant, with a degradation rate of 2.5(2) × 10^{13} molecules min^{-1} cm^{-2} when exposed to a 5-sun solar simulator, equipped with a UV cut-off filter. We therefore conclude that tantalum oxynitride thin films are able to act as self-cleaning coatings through visible light photocatalysis and that films of tantalum oxynitride can be synthesized using a scalable chemical vapour deposition route.

Introduction

In the materials chemistry community there have been significant developments in the use of metal oxynitrides as visible light activated photocatalysts,[1-4] with one of the earliest identified examples being tantalum oxynitride.[5] Research in this area has been driven by a motivation to develop a water splitting photocatalyst system - a combination of photocatalyst and co-catalysts - that can efficiently use solar energy to convert water into oxygen and hydrogen as a source of sustainable fuel and chemical feedstock.[6-10] The previous generation of metal oxide photocatalysts are unsuitable for solar fuel production as they can only be activated by UV light,[11] which makes up a small fraction of solar light. Due to this, the maximum solar to hydrogen efficiency for a UV photocatalyst is only 5%.[12] However, UV activated photocatalysts like titanium dioxide have found widespread commercial use in 'self-cleaning' applications,[13-14] antimicrobial coatings and in air purification.[15-16]

Absorption of light by the photocatalyst leads to formation of energetic electron-hole pairs, which can then migrate to the surface of the semiconductor. The photo-excited electron can reduce atmospheric oxygen to the superoxide radical, which then oxidises any organic species. The photo-generated holes meanwhile can oxidise surface bound water molecules, present under ambient conditions,[17] to surface bound hydroxide radicals, which can also then directly oxidise the organic pollutant. Evidence for this mechanism in is provided by quenching experiments conducted with titanium dioxide which show that the photocatalytic activity is retarded in the presence of hole and superoxide scavengers,[18-19] or in the absence of surface bound water.[20]

The question we pose in this paper is can the metal oxynitride visible light activated photocatalysts developed for water splitting also be used in self-cleaning coatings? Visible light activity would be highly desirable for self-cleaning applications because it would allow for their use in indoor environments, where UV activated photocatalysts cannot be used as the amount of UV light is negligible. In order to answer this question we have investigated the self-cleaning ability of tantalum oxynitride thin films, as an exemplar of the metal oxynitride visible light photocatalysts.

Tantalum (V) oxynitride, TaON, has been reported to crystallise in a number of structures. An alpha form was described by Buslaev, but has since been disproven.[21] The first

[a.] *School of Chemistry, University of Southampton, Southampton, UK, SO17 1BJ.*
[b.] *Kathleen Lonsdale Building, Department of Chemistry, University College London, Gordon Street, London, WC1H 0AJ, UK.*
[c.] *UK Catalysis Hub, Research Complex at Harwell, RAL, Oxford, OX11 0FA, UK*
[d.] *School of Chemistry, University of Leeds, Leeds, LS2 9JT, UK*
† Corresponding author. G.Hyett@soton.ac.uk
† Data associated with this publication is available. DOI:10.5258/SOTON/D0854
Electronic Supplementary Information (ESI) available: [details of any supplementary information available should be included here]. See DOI: 10.1039/x0xx00000x
† Footnotes relating to the title and/or authors should appear here.
Electronic Supplementary Information (ESI) available: [details of any supplementary information available should be included here]. See DOI: 10.1039/x0xx00000x

confirmed and most stable form is β-TaON which adopts the monoclinic *baddeleyite* structure, and unusually for an oxynitride has anion site ordering.[22] It has an experimentally determined direct band gap of 2.4 eV,[23] is yellow in colour and with band edges suitably aligned for both reduction of water to hydrogen and for generation of the oxygen radicals essential for the mechanism of self-cleaning.[24] Photocatalytic reduction of water by β-TaON under visible light irradiation has been repeatedly demonstrated.[7-8, 25-28] In terms of self-cleaning reactions, the decolouration of methylene blue has been reported for β-TaON,[29] but this is a two-electron reduction to a colourless form, rather than demonstration of complete oxidation of an organic contaminant.[14] Two meta stable phases have been convincingly reported: γ-TaON is orange, crystalizing in the monoclinic VO_2(B) structure;[30] δ-TaON adopts the anatase structure.[31] The gamma form has a smaller band gap of 2.15 eV, and has also demonstrated hydrogen evolution from methanol solution.[32] The gamma phase is formed by conversion of β-TaON at 850 °C under a high flow of ammonia.[30] The polymorphs of TaON can therefore easily be distinguished by their band gap and colour.

The majority of reported synthetic routes to powder TaON involve ammonolysis of tantalum oxide, but the exact conditions required have been a matter of some debate within the literature, with subtle differences in individual experimental setups producing different results, even with apparently equivalent reaction conditions.[33] This can be understood as the formation of TaON is a kinetically controlled process, with a competitive reaction between ammonia decomposition products favouring nitridation and in-situ produced water retarding it, where more 'aggressive' reaction conditions (higher temperature, longer reaction times) will lead to full nitridation to the more thermodynamically stable Ta_3N_5.[34-35] Some reports attempt to stabilize the formation of TaON through the introduction of a small partial pressure of water into the ammonia gas stream,[34, 36] with typical conditions being reaction at 850 °C for 10-15 hours.[7-8] However, TaON can also be synthesized using dry ammonia.[5, 31, 37-38]

Prior work on *thin films* of tantalum oxynitride has made use of a similar synthetic strategy to the work on powders, with the initial deposition of a tantalum oxide film followed by nitridation with ammonia. For example, anodization of tantalum foil yields a surface of tantalum oxide, which can be converted into tantalum oxynitride using dry ammonia at 700°C to 750 °C reacted for 3 to 6 hours.[26, 39] The shortened diffusion path into the thin film allows for faster reaction at lower temperature compared to the powder synthesis discussed above, but the cost of tantalum foil substrates limits the practicality of this approach. An alternative is to make use of magnetron sputtering to deposit a thin layer of tantalum metal onto a silica substrate, followed by annealing in air to tantalum oxide before the final ammonolysis step.[33] This has been achieved with wet ammonia at 750 °C.[25] Magnetron sputtering, using either DC or RF, can also be used to achieve direct formation of tantalum oxynitride without a high temperature ammonolysis step, though this requires the use of a tantalum metal target with a reactive gas mixture of oxygen, nitrogen and argon.[40-43] This allows deposition at much lower temperatures, from room temperature up to 100 °C, far lower than the temperature required for ammonolysis, but the films produced *via* the direct route tend to be amorphous. Finally, an approach has also been used through the synthesis of TaON powder and then electrophoretic deposition of the powder into a film.[27-28] This again has the advantage of being able to deposit at low temperature, but with the penalty of fragile, poorly adherent film formation.

In this work we demonstrate that it is possible to adapt the two-stage deposition process to make use of aerosol assisted chemical vapour deposition (AACVD) for the initial tantalum oxide film, which has advantages of scalability, film adhesion, and relatively low cost.[44-46] Sathasivam *et al* have demonstrated that thin films of amorphous Ta_2O_5 can be deposited using AACVD,[47] and we further show that subsequent ammonolysis at 700 °C allows for the formation of an amorphous tantalum oxynitride film which is able to use visible light for the complete photocatalytic destruction of a model pollutant.

Experimental Methods

Thin film synthesis

Thin films of tantalum oxynitride were deposited onto fused silica substrates in a two-stage process, with initial deposition of a film of tantalum oxide, followed by conversion to tantalum oxynitride through ammonolysis. The tantalum oxide thin films were deposited by AACVD using a cold walled reactor; details of the reactor have been published previously.[48]

Depositions were carried out from a solution of the tantalum (V) ethoxide in toluene using argon as a carrier gas. All precursor chemicals were handled under an atmosphere of argon (BOC, Pureshield) using standard Schlenk and glovebox techniques. Toluene (Fisher Scientific, reagent grade) was dried over 4 Å molecular sieves (Alfa Aesar, 3-5 mm beads). A stock solution of 0.25 M tantalum (V) ethoxide (Sigma Aldrich, 99.98%) was prepared in 20 ml of the dried toluene. In each deposition of tantalum oxide 2.5 ml of the 0.25 M tantalum (V) ethoxide stock was dissolved in a further 20 ml of dry toluene, from which an aerosol was generated using a piezoelectric humidifier (Maplin product no, L38K) and transported to the reactor under a 1.4 L min^{-1} flow of argon. Depositions were carried out onto fused silica (UQG optics, 10 x 25 x 1 mm^3) at a temperature of 425 °C. The reactor exhaust was connected to a silicone oil bubbler to prevent back diffusion of air into the reactor. The reaction was continued until no precursor solution remained, typically 45 mins.

For the second stage ammonolysis to form tantalum oxynitride, the tantalum oxide films were placed on top of a semi-circular carbon block inside a 35 mm diameter fused silica tube within a tube furnace, under a flow of ammonia. The carbon block was used as a substrate support and thermal mass to ensure that the substrate temperature would rapidly equilibrate with the furnace temperature. A silicone oil bubbler was again attached to the tube exhaust to prevent back-diffusion of air. In each experiment, a sample of tantalum oxide

coated substrate was heated at a steady rate of 7 °C min^{-1} under a flow of ammonia gas (0.1 L min, BOC Anhydrous) and then held at a temperature from 550 °C to 750 °C for 24 hours before being allowed to slowly cool to room temperature. Ammonia gas flow was maintained throughout the reaction and cool down period.

Thin film Characterisation

Grazing incident X-ray diffraction patterns were obtained using a Rigaku Smart Lab diffractometer equipped with a rotating anode Cu K_α source (45 kV, 200 mA), with data collected in the range 10° to 80° 2θ, with a step size of 0.02° and a collection time of 15 mins. Grazing incident scans were performed using an incident angle of 1° to minimize over penetration of the beam into the quartz substrate. Where appropriate, X-ray diffraction data were modelled using the GSAS suite of software packages with the EXPGUI graphical interface.[49-50]

Transmission spectroscopic data was collected for all deposited films in the range 200 nm to 2000 nm using a Perkin-Elmer Lambda 750S UV-Vis-NIR spectrometer equipped with a 100 mm integrating sphere. Imaging SEM was carried out on a FEI Nova 450 FEG-SEM operating at 5 kV and a working distance of 5 mm.

XAFS spectra of the thin films were recorded in fluorescence mode at the tantalum L_3 edge (9880 eV), on beamline B18 at the Diamond Light Source operating with a ring energy 3 GeV and at a current of 300 mA. The monochromator comprised a Si(111) crystal operating in Quick EXAFS mode. Calibration of the monochromator was carried out using a tantalum foil. Powder reference standards of Ta_2O_5, TaON and Ta_3N_5 were also measured. The Ta_2O_5 was purchased from Sigma Aldrich (99.9%) and used as supplied. Ta_3N_5 and TaON were synthesized by reaction of 0.8 g samples of Ta_2O_5 under a flow of dry ammonia at 900 °C for 24 hours, and a flow of wet ammonia at 900 °C for 16 hours, respectively. The powder reference samples were prepared as pellets by mixing the ground sample with cellulose to form a homogenous mixture, and then compressed using a pellet press and measured in transmission mode. A total of three spectra were averaged for each sample. The data were analysed using the Athena program.[51] The spectra were aligned using the tantalum foil response.

Photocatalytic Analysis

The photocatalytic activity of the deposited films was evaluated through the degradation of stearic acid under visible light irradiation.[52] A LOT-Oriel solar simulator with a 420 nm cut-off filter was used with a light intensity of 509 mW cm^{-2} **[Caution: solar simulators are intense UV sources that can cause skin and eye damage]**. In each experiment, a thin layer of stearic acid (98%, Fisher Scientific) was dip-coated onto the tantalum oxynitride film from a 0.05 M solution of stearic acid in dichloromethane (99.8%, Fisher Scientific). The amount of stearic acid deposited was quantified using FTIR, recorded using a Perkin Elmer 100 spectrometer over the range 2800 cm^{-1} to 3000 cm^{-1}, using the previously established relationship that 1 cm^{-1} of integrated peak intensity is equivalent to 9.7×10^{15} molecules of stearic acid.[53] Once the stearic acid layer had been applied and quantified the sample was placed under the filtered solar simulator for exposure to visible light. The sample was then removed every 30 mins to monitor the photocatalytic degradation of the stearic acid layer, up to a total of 210 mins of exposure.

Results

Initial film deposition onto the fused silica substrates was carried out using AACVD of tantalum ethoxide from toluene solution at 425 °C. This yielded a transparent film, with the presence of a weak interference colour on the surface when observed in reflection. Analysis by GI-XRD found the presumed films of tantalum oxide to be amorphous, as identified in prior work.[47] One sample was annealed under inert atmosphere at 900 °C, and this was found to have crystallised the sample, such that the diffraction pattern could be indexed to Ta_2O_5. This diffraction data can be found in the supplementary information (Figure S1). Samples of amorphous tantalum oxide film were reacted with ammonia at temperatures of 550 °C, 600 °C, 650 °C, 700 °C and 750 °C for 24 hours. There were no observable changes in the film annealed at 550 °C, but the films annealed at 600 °C and higher temperatures appeared orange-brown, with the colour intensity increasing with temperature, up to the film annealed at 750 °C, which was bright red. These ammonia annealed films were characterized using GI-XRD, UV-vis spectroscopy and XAFS and assessed for photocatalytic activity.

Grazing Incidence X-ray diffraction

The grazing incident angle X-ray diffraction data collected on the samples annealed under ammonia up to 700 °C showed no Bragg peaks across the range of 10° to 80° 2θ, instead broad features were observed in the background indicative of amorphous or poorly crystalline phases. These diffraction patterns can be found in Figure 1a. The exception to this was the sample annealed at 750 °C. This had sharp Bragg peaks that could be indexed to orthorhombic Ta_3N_5 (ICSD 16253). A Rietveld refinement was carried out in the *Cmcm* space group against this data and provided a good fit to the published Ta_3N_5 structure with no preferred orientation, as shown in figure 1b. Lattice parameters of a = 3.88(1) Å, b =10.21(1) Å and c = 12.27(1) Å were found, consistent with previously reported values.

Compositional analysis using XAFS

X-ray absorption spectra were collected in fluorescence mode on thin film samples and in transmission for foil and powder standards. The composition of the powder standards was confirmed using X-ray diffraction. Figure 2 illustrates the characteristic Ta-L_3 edge XANES spectra of Ta foil, Ta_2O_5, TaON and Ta_3N_5 standard compounds together with that for the thin film samples annealed under ammonia. By using the maximum of the derivative as the edge position, the edge of the tantalum foil was located at 9881 eV. The edge position for the ammonia

annealed thin films corresponded to ~9883 eV, which matches the value found for the different tantalum reference compounds, confirming the presence of tantalum (V) in the thin films. In order to identify and to quantify the composition of the annealed thin films, XANES data were analysed by Linear Combination Fitting (LCF). This led to the estimated compositions shown in table 1. The LCF fits for all of the samples can also be found in Figure S2. The analysis shows that at the lower temperatures from 550 °C to 650 °C there is only partial conversion of the tantalum oxide to tantalum oxynitride, with the TaON fraction increasing with temperature from 28.4 % to 70.1 %. At 700 °C there is almost complete conversion to TaON at 98.3 % with the remaining tantalum present as Ta_3N_5. The sample annealed at 750 °C is found to be composed exclusively of Ta_3N_5, in agreement with the XRD analysis.

Composition of the films was further confirmed by looking at the Fourier transforms of the EXAFS data. Figure 3a shows a good match between the Fourier transforms of the NH_3 annealed sample at 750 °C and that of Ta_3N_5; whereas the Fourier transform of the sample annealed at 550 °C no longer matches that of Ta_2O_5 (Figure 3b).

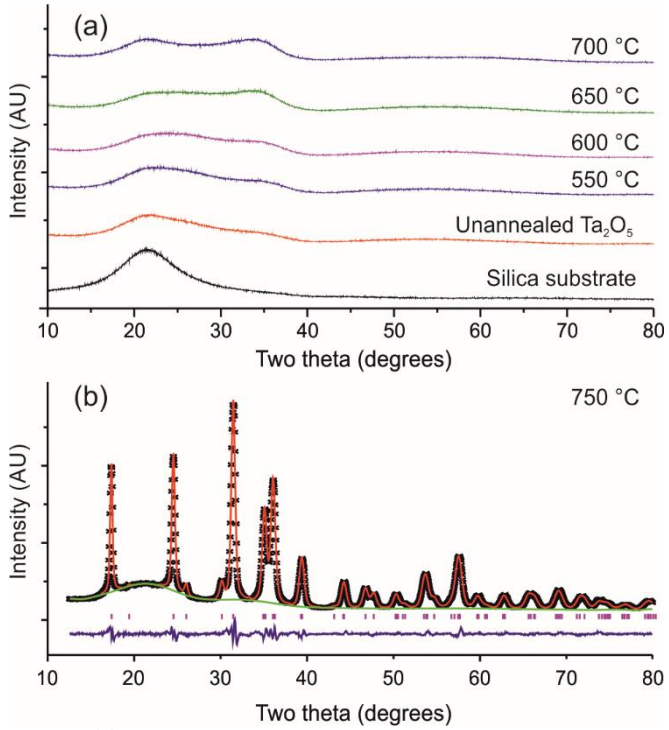

Figure 1. (a) X-ray diffraction patterns collected from a range of samples. In ascending order: an uncoated silica substrate; an as deposited tantalum oxide film and films annealed under ammonia at 550 °C, 600 °C, 650 °C and 700 °C. **(b)** Diffraction pattern collected on sample annealed under ammonia at 750 °C showing Bragg reflections. Data is shown with black crosses, and has been modelled using Rietveld refinement (red line). Tick marks indicate expected positions for the *Cmcm* Ta_3N_5 and the bottom blue trace is the difference plot between the model and the data.

Ammonia Anneal Temp.	Fractional Composition from LCF			Film Thickness from SEM
	Ta_2O_5	TaON	Ta_3N_5	
550 °C	71.6 %	28.4 %	0 %	230 nm
600 °C	58.4 %	41 %	0 %	250 nm
650 °C	29.9 %	70.1 %	0 %	200 nm
700 °C	0 %	98.3 %	1.7 %	280 nm
750 °C	0 %	0 %	100 %	380 nm

Table 1. Results of linear combination fit analysis of XANES spectra of confirmed Ta_2O_5, TaON and Ta_3N_5 to the XANES spectra of the tantalum oxide films annealed under ammonia at 550 °C to 750 °C.

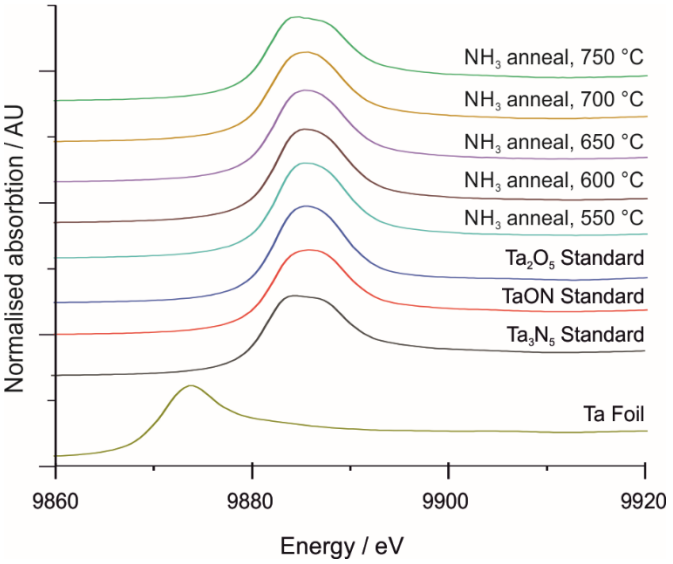

Figure 2. XANES spectra of the Ta-L_3 edge, for reference tantalum foil; standard tantalum oxide, tantalum oxynitride and tantalum nitride powders; and tantalum oxynitride thin films annealed at 550 °C to 750 °C.

UV-vis spectroscopy and SEM

Transmission spectra were recorded for all tantalum oxynitride films and an amorphous tantalum oxide film. Plots of these data can be found in Figure S3. The spectra show a steadily shifting absorption edge with ammonolysis temperature, leading to increasing absorption of visible light. Tauc plots calculated from this data are shown in figure 4, and have been used to estimate the band gap of the materials, assuming direct band gaps. The analysis gives a value of 4.13 eV for the amorphous oxide, and values of 3.66 eV and 3.36 eV for the films annealed at 550 °C and 600 °C in ammonia. These values all fall within the UV, although the Tauc plot for the film annealed at 600 °C has a tail of absorbance stretching into the visible, which explains the pale brown colour of the film observed by eye. For the films annealed at 650 °C and 700 °C we see a significant reduction in band gap to 2.63 eV and 2.58 eV, consistent with the darker coloration observed visually in these films. Finally, the sample annealed under ammonia at 750 °C has as a band gap of 2.18 eV.

Side-on SEM images allowed the film thickness of the samples to be estimated. This found the films to be between 200 and 380 nm thick, as reported in table 1. The images can be found in Figure S4. The top-down images revealed the films annealed under ammonia up to 700 °C to have identical morphology, very smooth, lacking any surface features and

composed of amorphous particles of less than 50 nm in diameter. The film annealed at 750 °C, which crystallised, developed minor surface cracks, and the appearance of domains on the order of 500 nm. The images can be seen in figure S5.

Photocatalysis

The self-cleaning ability of the tantalum oxynitride films was assessed using the stearic acid test.[51] An approximate 35 nm layer of stearic acid was dip coated onto the films, and the thickness of this quantified using FTIR in the region of 2800 cm^{-1} to 3000 cm^{-1}, where the C-H stretching peaks are found. The stearic acid coated films were then exposed to a 5-sun solar simulator light source equipped with a 420 nm cut off filter, which provided a visible light source with an intensity of approximately 500 $mWcm^{-2}$.

Table 2. Summary of composition, band gap and photocatalytic activity for the tantalum oxynitride films

Anneal Temp.	Est. Composition	Band Gap (eV)	1st order rate constant (min^{-1})	Initial rate (molecules cm^{-2} min^{-1})
None	Uncoated Control	-	$1.6(9) \times 10^{-4}$	$1.2(7) \times 10^{12}$
None	Amorphous Ta_2O_5	4.13	$1.8(9) \times 10^{-4}$	$1.3(7) \times 10^{12}$
550 °C	$Ta_2O_{5-x}N_x$	3.66	$2.4(6) \times 10^{-4}$	$1.7(4) \times 10^{12}$
600 °C	$Ta_2O_{5-x}N_x$	3.36	$4.2(0.6) \times 10^{-4}$	$3.6(6) \times 10^{12}$
650 °C	$Ta_2O_{5-x}N_x$+TaON	2.63	$25(2) \times 10^{-4}$	$18(2) \times 10^{12}$
700 °C	TaON	2.58	$33(1) \times 10^{-4}$	$25(2) \times 10^{12}$
750 °C	Ta_3N_5	2.18	$3(1) \times 10^{-4}$	$2.1(7) \times 10^{12}$

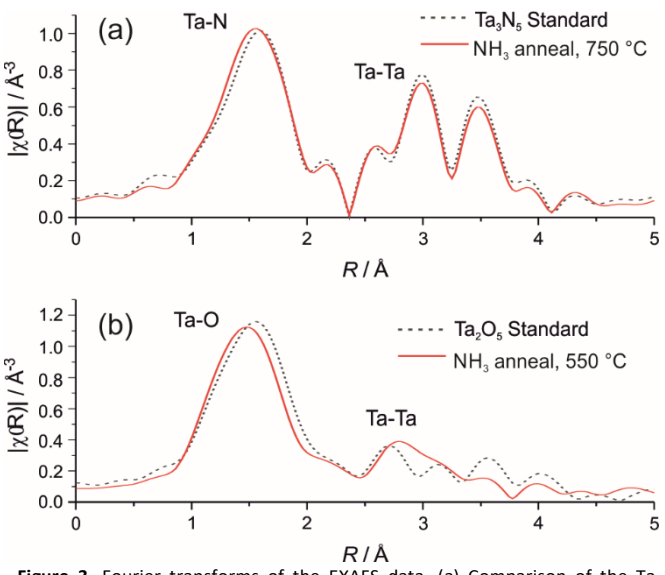

Figure 3. Fourier transforms of the EXAFS data. (a) Comparison of the Ta_3N_5 standard with the film annealed at 750°C. Annotation marks expected position of the Ta-N and Ta-Ta distances. (b) Similar comparison of Ta_2O_5 standard with the film annealed at 550°C

The photocatalytic degradation of the stearic acid layer was monitored by re-recording the FTIR spectra every 30 mins for a total of 210 mins. An uncoated silica substrate was also tested as a control. Example spectra recorded on the film annealed at 700°C can be seen in figure 5. Plots of the stearic acid concentration as a function of time for the tantalum oxynitride films can also be seen in Figure 5. These show little or no photocatalytic degradation, within the margin of error, for the amorphous tantalum oxide, and tantalum oxynitride films annealed under ammonia at the lowest temperatures (550 °C and 600 °C) and at the highest temperature, 750 °C. However, the data for the films annealed under ammonia at 650 °C and 700 °C show clear degradation within 3 hours, and the expected first order kinetics.[13] First order rate constants for all data sets have been calculated, and these are shown in table 2 alongside the initial rate values. Analysis of the control provides a background rate of $1.6(9) \times 10^{-4}$ min^{-1}. For the amorphous Ta_2O_5 film a rate of $1.8(9) \times 10^{-4}$ min^{-1} is observed, within error of background rate, indicating the expected absence of visible light photocatalytic activity. For the films films annealed at the highest and lowest temperatures, 550 °C and 750 °C, there is negligible degradation over the 3.5-hour experimental run time, with rate constants of $2.4(6) \times 10^{-4}$ min^{-1} and $3(1) \times 10^{-4}$ min^{-1} respectively, which provide only tentative evidence of minimal visible light photocatalysis. In contrast, for the film annealed at 600 °C there is small but measureable degradation with a first order rate of $4.2(6) \times 10^{-4}$ min^{-1}. For the films annealed at 650 °C and 700 °C these rates are an order of magnitude higher with values 25(2) and $33(1) \times 10^{-4}$ min^{-1} respectively, with almost 50% of the stearic acid layer being removed within 3.5 hours.

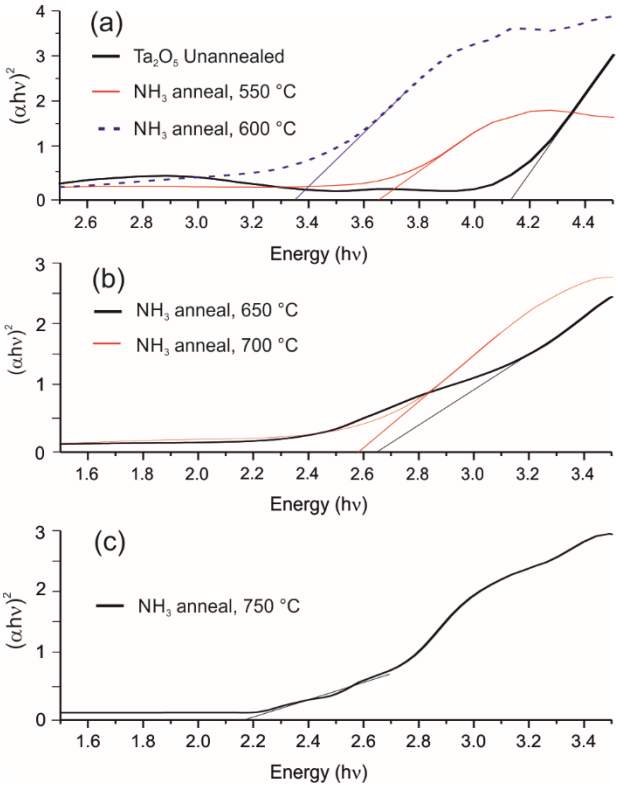

Figure 4. Tauc plots for (a) unannealed Ta_2O_5 sample, and samples annealed under ammonia at 550 °C and 600 °C (b) annealed at 650 °C and 700 °C (c) annealed at 750 °C.

Discussion

It has been shown that AACVD can be used to deposit tantalum oxide,[47] and our results clearly show that these can then be annealed under ammonia to introduce nitrogen into the lattice. The most easily characterised of these samples is the film annealed at 750 °C. This has a crystalline diffraction pattern that can be modelled as originating from Ta_3N_5, and this result is supported by the EXAFS fitting which provides an excellent match to the Ta_3N_5 standard. The spectroscopic data indicates a band gap of 2.18 eV which is a good match to the previously reported value of 2.1 eV for tantalum nitride. Although the sample can absorb visible light, the absence of visible light photocatalysis highlighted by the samples inability to degrade stearic acid can be understood from the point of view that this band gap is too small and the band edges have insufficient energy to catalyse the required redox reactions for self-cleaning activity.

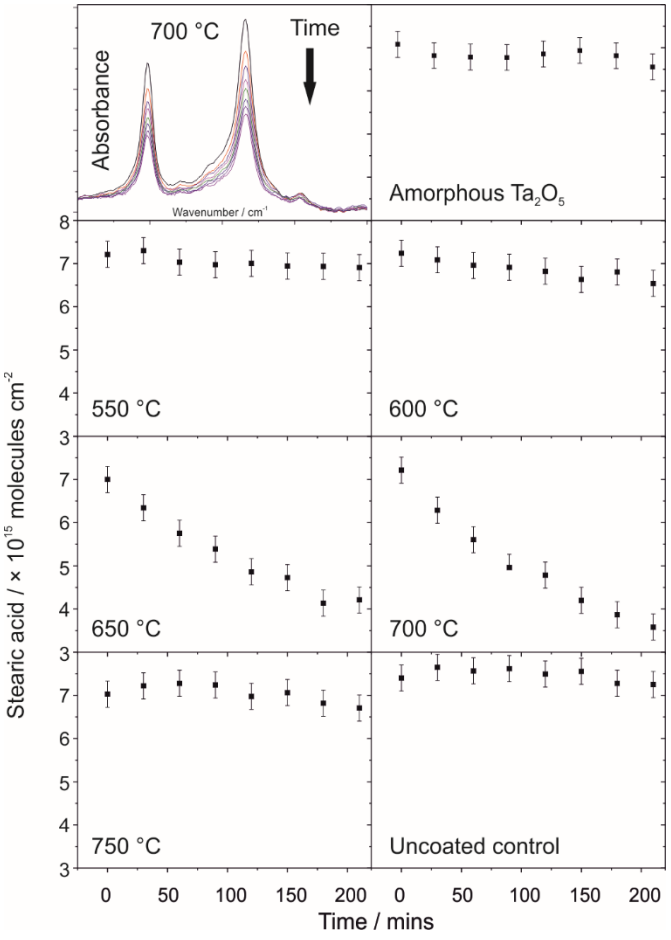

Figure 5. (Top left) Example FTIR spectra of the C-H stretching peaks of stearic acid layer on tantalum oxynitride film annealed at 700 °C, showing destruction of stearic acid as a function of time. (Top right onwards) Plots of stearic acid layer as a function of time for all five tantalum oxynitride films and for an uncoated control silica sample.

The lack of crystallinity in the remaining samples makes the characterisation more challenging. Previous work by Taviot-Gueho *et al* on tantalum oxynitride films deposited using reactive magneton sputtering suggests that lack of Bragg peaks is not indicative of a truly amorphous TaO_xN_y phase, but it is more likely that the samples are formed of mixtures of "crystalline domains of a few tens of angstroms diameter".[54] In their work the changing oxygen to nitrogen ratio of samples made under more nitriding conditions is not interpreted as changing composition of a single phase, but instead as a changing nanoscopic mixture of the bulk stable phases Ta_2O_5, TaON and Ta_3N_5. This is consistent with the consensus within the literature that nitridation of tantalum oxide is a kinetic process which proceeds via a successive transformation from Ta_2O_5 to TaON through to Ta_3N_5, with transitional stages of nitrogen doped Ta_2O_5 and oxygen doped Ta_3N_5.[5, 25, 34-35] Considering this analysis of previously investigated amorphous samples, we can now attempt to interpret the results of our tantalum oxynitride thin films. The spectroscopic data of the sample annealed at the lowest temperature of 550 °C indicates a band gap that has reduced compared to the oxide, but still falls outside the visible at 3.6 eV. Considering this value the EXAFS data is better interpreted as a sample at the early stages of nitridation, and composed of nitrogen doped tantalum oxide, rather than a mixture of Ta_2O_5 and TaON. A similar interpretation is also valid for the sample annealed at 600°C, although with a higher nitrogen content determined from fitting of EXAFS data and a further reduction in the band gap to 3.4 eV. It is also likely that this sample does contain a small fraction of TaON, due to the limited visible light photocatalytic activity observed.

Films of tantalum oxide has been shown to be photocatalytic under UV light,[47] however in contrast we show that amorphous tantalum oxide is not active under visible light alone, and that only after nitridation can activity be observed using a 420 nm cut-off filter. Both films prepared at 650 °C and 700 °C show clear visible light activated photocatalytic degradation of stearic acid, and both spectroscopic and EXAFS data support the conclusion that these films contain significant amounts of TaON. The band gaps of 2.63 eV and 2.58 eV provide a reasonable match to the value of 2.4 eV previously reported for TaON,[24] and the EXAFS suggest a composition of 70.1% TaON for the film annealed at 650 °C, and 98.3% for the film annealed at 700 °C. Surface roughness, morphology and film thickness can affect photocatalytic rate, but the SEM images (Figure SX) reveal that all the amorphous films have identical surface morphology, and a thickness between 200-300nm. The greater rate observed for the sample at 700 °C is therefore consistent with this sample being almost pure TaON, with the imperfect conversion at 650 °C leading to lower photocatalytic rate simply due to a reduction in the surface concentration of the active phase.

We can conclude from this that the ideal synthetic conditions in our study are to anneal tantalum oxide under ammonia at 700 °C for 24 hours. This leads to a film which can degrade stearic acid with an initial rate of $25(2) \times 10^{12}$ molecules min^{-1} cm^{-2} and a first order rate constant of $33(1) \times 10^{-4}$ min^{-1} under five-sun solar simulation. The loading of stearic acid used in the photocatalytic test above is equivalent to 3.3×10^{-6} g cm^{-2}.

In an attempt to estimate real-world loadings of greasy organics on a surface, we contaminated a series of substrates

with greasy fingerprints and used FTIR to model the loading, which produced an average of 4×10^{-6} g cm^{-2}. Thus, the contaminant loading of our test is equivalent to the challenge that would be experienced under actual conditions. However, the light intensity used at 500 mW cm^{-2} is significantly higher than would be experienced in real conditions. Bright sunlight is of the order of 100 mW cm^{-2}, thus assuming a linear photocatalytic dependence on light intensity, our most active film would be able to self-clean in approximately 28 hours in outdoor conditions, or indoors under direct sunlight. However for indoor areas under artificial light alone, typical intensity is far lower, 0.50 to 0.01 mW cm^{-2}, so for these areas we would not expect to be able to observe reasonable activity. One caveat to this is that photocatalytic rates do not necessarily decline linearly with light intensity but instead are proportional to the square root of light intensity for reactions that involve slow charge transfer processes - as the rate is typically limited by the recombination of electron-hole carriers rather than surface redox reactions.[55] Therefore, our photocatalyst may perform better than expected under direct sunlight, although for indoor lighting alone the rate will probably remain too low.

There have been some prior examples of stearic acid degradation by visible light. Films of nitrogen dope titanium dioxide have been reported to degrade stearic acid (rate of 0.13×10^{12} molecules min^{-1} cm^{-2}) using a fluorescent light source, although some of this activity may have come from potential leakage of UV light through the fluorescent coating.[56] Unambiguous evidence of visible light degradation has been reported with nano-particulate silver coated titania thin films, where with cut off filters rate as high as 1.0×10^{12} molecules min^{-1} cm^{-2} have been observed.[57,58] These experiments were conducted with lower intensity light sources than that used for the experiments on the TaON film presented here (rate of 25×10^{12} molecules min^{-1} cm^{-2}), indicating that under similar conditions the Ag-TiO_2 films are likely to have equivalent degradation rates.

We can also compare our results to UV photocatalysts. Titanium dioxide is the most widely tested and one of the most active UV photocatalysts, although this is most often tested using narrow spectrum UV light, the intensity used is typically equivalent to the UV found in bright unfiltered sunlight ~5 $mWcm^{-2}$. Under these conditions, initial rates of 5.8×10^{12} molecules $min^{-1}cm^{-2}$ to 6.2×10^{13} molecules $min^{-1}cm^{-2}$ are observed which would lead to an estimated destruction of a stearic acid layer of 4×10^{-6} g cm^{-2} in 2.3 to 24 hours under direct sunlight, [59-63] compared to an estimated 28 hours for our TaON film. Therefore, for direct sunlight photocatalysis titanium dioxide remains the more viable choice, but for indoor areas where glass windows or roofs filter the UV portion of sunlight, the rates presented here for tantalum oxynitride are viable.

Conclusions

In this paper we have shown that films of tantalum oxynitride can be used for direct and complete degradation of stearic acid. This is an excellent model for the greasy, lipid-like organic pollutants that are encountered on the contaminated surfaces where self-cleaning coatings are required. The rates observed are sufficiently high that the use of tantalum oxynitride in direct sunlight is viable, even where the UV component has been filtered. We have also demonstrated that the photocatalytically active tantalum oxynitride films can be made using a scalable chemical vapour deposition route.

Conflicts of interest

There are no conflicts to declare.

Acknowledgements

The acknowledgements come at the end of an article after the conclusions and before the notes and references. V.C. kindly thanks the UK Catalysis Hub for resources and support provided via the membership of the UK Catalysis Hub Consortium and funded by EPSRC (EPSRC grants EP/K014706/1 and EP/K014714/1). The authors wish to acknowledge the Diamond Light Source for provision of beamtime (SP15151). We also wish to thank the Leverhulme Trust for funding through RPG-2014-204.

Notes and references

1. M. Ahmed, G. Xinxin, *Inorganic Chemistry Frontiers,* 2016, 578-590.
2. K. Maeda, K. Domen, *Mrs Bulletin,* 2011, **36**, 25-31.
3. C. Pan, T. Takata, K. Kumamoto, S.S. Khine Ma, K. Ueda, T. Minegishi, M. Nakabayashi, T. Matsumoto, N. Shibata, Y. Ikuhara, K. Domen, *Journal of Materials Chemistry A,* 2016, **4**, 4544-4552.
4. P.-T.C. Le, A. Ishikawa, A. Ziani, G.L. Le, M. Yoshida, J. Kubota, F. Tessier, K. Domen, *J. Phys. Chem. C,* 2009, **113**, 6156-6162.
5. G. Hitoki, T. Takata, J.N. Kondo, M. Hara, H. Kobayashi, K. Domen, *Chem. Commun.,* 2002, 1698-1699.
6. D.M. Fabian, S. Hu, N. Singh, F.A. Houle, T. Hisatomi, K. Domen, F. Osterloh, S. Ardo, *Energy & Env. Sci.,* 2015, 2852-2850.
7. M. Hara, T. Takata, J.N. Kondo, K. Domen, *Catal. Today,* 2004, **90**, 313-317.
8. D. Yamasita, T. Takata, M. Hara, J.N. Kondo, K. Domen, *Solid State Ionics,* 2004, **172**, 591-595.
9. K. Maeda, T. Takata, M. Hara, N. Saito, Y. Inoue, H. Kobayashi, K. Domen, *J. Am. Chem. Soc.,* 2005, **127**, 8286-8287.
10. C. Zhen, R. Chen, L. Wang, G. Liu, H.-M. Cheng, *Journal of Materials Chemistry A,* 2016, **4**, 2783-2800.
11. F.E. Osterloh, *Chem. Mater.,* 2008, **20**, 35-54.
12. J.R. Bolton, S.J. Strickler, J.S. Connolly, *Nature,* 1985, **316**, 495-500.
13. A. Mills, A. Lepre, N. Elliott, S. Bhopal, I.P. Parkin, S.A. O'neill, *J. Photochem. Photobiol., A,* 2003, **160**, 213-224.
14. A. Mills, C. Hill, P.K.J. Robertson, *J. Photochem. Photobiol., A,* 2012, **237**, 7-23.
15. A. Mills, S. Elouali, *J. Photochem. Photobiol., A,* 2015, **305**, 29-36.

16. K. Sunada, T. Watanabe, K. Hashimoto, *J. Photochem. Photobiol., A,* 2003, **156**, 227-233.
17. G. Munuera, F.S. Stone, *Discussions of the Faraday Society,* 1971, 205-214.
18. D. Wu, B. Wang, W. Wang, T. An, G. Li, T.W. Ng, H.Y. Yip, C. Xiong, H.K. Lee, P.K. Wong, *Journal of Materials Chemistry A,* 2015, **3**, 15148-15155.
19. L. Ye, Y. Su, X. Jin, H. Xie, C. Zhang, *Environmental Science: Nano,* 2014, **1**, 90-112.
20. L.A. Dibble, G.B. Raupp, *Catal. Lett.,* 1990, **4**, 345-354.
21. M.-W. Lumey, R. Dronskowski, *Z. Anorg. Allg. Chem.,* 2003, **629**, 2173-2179.
22. D. Armytage, B.E.F. Fender, *Acta Crystallogr., Sect. B: Struct. Sci.,* 1974, **B 30**, 809-812.
23. E. Orhan, F. Tessier, R. Marchand, *Solid State Sci.,* 2002, **4**, 1071-1076.
24. W.-J. Chun, A. Ishikawa, H. Fujisawa, T. Takata, J.N. Kondo, M. Hara, M. Kawai, Y. Matsumoto, K. Domen, *The Journal of Physical Chemistry B,* 2003, **107**, 1798-1803.
25. A. Dabirian, H.V.T. Spijker, R. Van De Krol, *Energy Procedia,* 2012, **22**, 15-22.
26. J. Hou, C. Yang, H. Cheng, S. Jiao, O. Takeda, H. Zhu, *Energy & Env. Sci.,* 2014, **7**, 3758-3768.
27. M. Higashi, K. Domen, R. Abe, *J. Am. Chem. Soc.,* 2012, **134**, 6968-6971.
28. M. Higashi, K. Domen, R. Abe, *Energy & Env. Sci.,* 2011, **4**, 4138-4147.
29. J.H. Hsieh, C. Li, H.C. Liang, *Thin Solid Films,* 2011, **519**, 4699-4704.
30. H. Schilling, A. Stork, E. Irran, H. Wolff, T. Bredow, R. Dronskowski, M. Lerch, *Angew. Chem. Int. Edit.,* 2007, **46**, 2931-2934.
31. T. Ludtke, A. Schmidt, C. Gobel, A. Fischer, N. Becker, C. Reimann, T. Bredow, R. Dronskowski, M. Lerch, *Inorg. Chem.,* 2014, **53**, 11691-11698.
32. Z. Wang, J.G. Hou, C. Yang, S.Q. Jiao, K. Huang, H.M. Zhu, *Energy & Env. Sci.,* 2013, **6**, 2134-2144.
33. M. De Respinis, M. Fravventura, F.F. Abdi, H. Schreuders, T.J. Savenije, W.A. Smith, B. Dam, R. Van De Krol, *Chem. Mater.,* 2015, **27**, 7091-7099.
34. M. Harb, P. Sautet, E. Nurlaela, P. Raybaud, L. Cavallo, K. Domen, J.-M. Basset, K. Takanabe, *Phys. Chem. Chem. Phys.,* 2014, **16**, 20548-20560.
35. M. Hara, E. Chiba, A. Ishikawa, T. Takata, J.N. Kondo, K. Domen, *J. Phys. Chem. B,* 2003, **107**, 13441-13445.
36. A. Dabirian, R. Van De Krol, *Chem. Mater.,* 2015, **27**, 708-715.
37. M. Hara, G. Hitoki, T. Takata, J.N. Kondo, H. Kobayashi, K. Domen, *Catal. Today,* 2003, **78**, 555-560.
38. R. Nakamura, T. Tanaka, Y. Nakato, *The Journal of Physical Chemistry B,* 2005, **109**, 8920-8927.
39. S. Banerjee, S.K. Mohapatra, M. Misra, *Chem. Commun.,* 2009, 7137-7139.
40. J.H. Hsieh, C.C. Chang, Y.K. Chang, J.S. Cherng, *Thin Solid Films,* 2010, **518**, 7263-7266.
41. D. Cristea, A. Crisan, N. Cretu, J. Borges, C. Lopes, L. Cunha, V. Ion, M. Dinescu, N.P. Barradas, E. Alves, M. Apreutesei, D. Munteanu, *Appl. Surf. Sci.,* 2015, **354**, 298-305.
42. D. Cristea, D. Constantin, A. Crisan, C.S. Abreu, J.R. Gomes, N.P. Barradas, E. Alves, C. Moura, F. Vaz, L. Cunha, *Vacuum,* 2013, **98**, 63-69.
43. A. Bousquet, F. Zoubian, J. Cellier, T. Sauvage, E. Tomasella, *Plasma Processes and Polymers,* 2013, **10**, 990-998.
44. C.E. Knapp, C.J. Carmalt, *Chem. Soc. Rev.,* 2016, **45**, 1036-1064.
45. M.J. Powell, C.J. Carmalt, *Chemistry – A European Journal,* 2017, **23**, 15543-15552.
46. P. Marchand, I.A. Hassan, I.P. Parkin, C.J. Carmalt, *Dalton Trans.,* 2013, **42**, 9406-9422.
47. S. Sathasivam, B.a.D. Williamson, A. Kafizas, S.A. Althabaiti, A.Y. Obaid, S.N. Basahel, D.O. Scanlon, C.J. Carmalt, I.P. Parkin, *J. Phys. Chem. C*, 2017, **121**, 202-210.
48. K. Rees, E. Lorusso, S.D. Cosham, A.N. Kulak, G. Hyett, *Dalton Trans.,* 2018, **47**, 10536-10543.
49. A.C. Larson, R.B. Von Dreele, *Los Alamos National Laboratory Report LAUR,* 2000, 86-748.
50. B.H. Toby, *J. Appl. Crystallogr.,* 2001, **34**, 210-213.
51. B. Ravel, M. Newville, *Journal of Synchrotron Radiation,* 2005, **12**, 537-541.
52. P. Sawunyama, L. Jiang, A. Fujishima, K. Hashimoto, *J. Phys. Chem. B,* 1997, **101**, 11000-11003.
53. A. Mills, J. Wang, *J. Photochem. Photobiol., A,* 2006, **182**, 181-186.
54. C. Taviot-Guého, J. Cellier, A. Bousquet, E. Tomasella, *The Journal of Physical Chemistry C,* 2015, **119**, 23559-23571.
55. T. Minabe, D.A. Tryk, P. Sawunyama, Y. Kikuchi, K. Hashimoto, A. Fujishima, *J. Photochem. Photobiol., A,* 2000, **137**, 53-62.
56. R. Quesada-Cabrera, C. Sotelo-Vázquez, M. Quesada-González, E.P. Melián, N. Chadwick, I.P. Parkin, *J. Photochem. Photobiol., A*, 2017, **333**, 49-55.
57. A. Kafizas, S. Kellici, J.A. Darr, I.P. Parkin, *J. Photochem. Photobiol., A*, 2009, **204**, 183-190.
58. C.W. Dunnill, K. Page, Z.A. Aiken, S. Noimark, G. Hyett, A. Kafizas, J. Pratten, M. Wilson, I.P. Parkin, *J. Photochem. Photobiol., A*, 2011, **220**, 113-123.
59. A. Kafizas, C.W. Dunnill, I.P. Parkin, *Phys. Chem. Chem. Phys.,* 2011, **13**, 13827-13838.
61. N.J. Platt, K.M. Kaye, G.J. Limburn, S.D. Cosham, A.N. Kulak, R.G. Palgrave, G. Hyett, *Dalton Trans.,* 2017, **46**, 1975-1985.
61. J.S. Park, W. Choi, *Langmuir,* 2004, **20**, 11523-11527.
62. V. Pore, A. Rahtu, M. Leskelä, M. Ritala, T. Sajavaara, J. Keinonen, *Chem. Vap. Deposition,* 2004, **10**, 143-148.
63. R. Quesada-Cabrera, C. Sotelo-Vazquez, J.A. Darr, I.P. Parkin, *Applied Catalysis B: Environmental,* 2014, **160–161**, 582-588.

